

Scaling of quadratic and linear magneto-optic Kerr effect spectra with L₂₁ ordering of Co₂MnSi Heusler compound

Robin Silber,^{1,2,3} Daniel Král,⁴ Ondřej Stejskal,^{2,4} Takahide Kubota,⁵ Yasuo Ando,⁶ Jaromír Pištora,^{1,2} Martin Veis,⁴ Jaroslav Hamrle,⁴ and Timo Kuschel³

¹*Nanotechnology Centre, VŠB-Technical University of Ostrava, Ostrava, Czech Republic*

²*IT4Innovations, VŠB-Technical University of Ostrava, Ostrava, Czech Republic*

³*Department of Physics, Bielefeld University, Bielefeld, Germany*

⁴*Faculty of Mathematics and Physics, Charles University, Prague, Czech Republic*

⁵*Institute for Materials Research, Tohoku University, Sendai, Japan*

⁶*Department of Applied Physics, Tohoku University, Sendai, Japan*

The Heusler compound Co₂MnSi provides a crystallographic transition from B2 to L₂₁ structure with increasing annealing temperature T_a , being a model system for investigating the influence of crystallographic ordering on structural, magnetic, optic, and magneto-optic (MO) properties. Here, we present quadratic magneto-optic Kerr effect (QMOKE) spectra depending on M^2 in addition to the linear magneto-optic Kerr effect (LinMOKE) spectra being proportional to M , both in the extended visible spectral range of light from 0.8 eV to 5.5 eV. We investigated a set of Co₂MnSi thin films deposited on MgO(001) substrates and annealed from 300°C to 500°C. The amplitude of LinMOKE and QMOKE spectra scales linearly with T_a , and this effect is well pronounced at the resonant peaks below 2.0 eV of the QMOKE spectra. Furthermore, the spectra of the MO parameters, which fully describe the MO response of Co₂MnSi up to the second order in M , are obtained dependent on T_a . Finally, the spectra are compared to ab-initio calculations of a purely L₂₁ ordered Co₂MnSi Heusler compound.

Heusler compounds are a class of materials with many intriguing properties which keep them still in the focus of active research nowadays¹. The Co₂MnSi Heusler compound is demonstrated to be a half-metallic ferromagnet^{2–4} with a band gap of 0.4 to 0.8 eV^{5,6} and a Curie temperature of 985 K⁷. It is well-known that the magnetic properties of Heusler compounds strongly depend on the crystallographic ordering⁸. The Heusler compound Co₂MnSi is a good model system as it provides transition from B2 to L₂₁ crystallographic ordering with increasing annealing temperature T_a ^{9,10}. The L₂₁ structure refers to a perfectly ordered crystal, whose two Co sublattices are at 8c Wyckoff positions ($\frac{1}{4}, \frac{1}{4}, \frac{1}{4}$), whereas Mn and Si occupy the 4a (0,0,0) and 4b ($\frac{1}{2}, \frac{1}{2}, \frac{1}{2}$) positions, respectively¹¹. The B2 structure refers to lower ordering, for which interchange of atoms between Mn and Si sublattices occurs.

The magneto-optic Kerr effect (MOKE), including linear MOKE (LinMOKE) and quadratic MOKE (QMOKE), has been routinely used at single wavelengths in investigations of magnetic properties, composition or ordering of Heusler compounds^{9–19}. In the study carried out by Wolf *et al.*¹⁰, the dependence of LinMOKE and QMOKE on crystallographic ordering of the Co₂MnSi Heusler compound has been studied at single wavelength 638 nm. Here, we investigate LinMOKE with in-plane magnetization parallel to the plane of incidence (longitudinal MOKE, LMOKE) spectroscopy and QMOKE spectroscopy^{20,21} in the spectral range of 0.8–5.5 eV. In our work, we focus on two features: (i) the QMOKE spectra show unusual oscillations for the photon energies of extended visible spectral range (ii) the LinMOKE and QMOKE scale with T_a .

To study this behaviour with respect to the material

properties of the Co₂MnSi Heusler compound, the magneto-optic (MO) parameters K , G_s and $2G_{44}$ ^{21,22} (fully describing the MO response of cubic crystal structures up to the second order in magnetization M) are obtained from the LMOKE and QMOKE spectra. The spectra of the diagonal permittivity ϵ_d of 0th order (independent from M), measured by ellipsometry, are also included. Furthermore, all the experimental results are accompanied by and compared to theoretical ab-initio calculations for L₂₁ crystallographic ordering.

Each of the studied samples consists of a 30 nm-thick Co₂MnSi layer epitaxially grown by inductively coupled plasma-assisted magnetron sputtering on a single crystalline MgO(001) substrate buffered with a 40 nm thick Cr layer. The samples are capped with a 1.3 nm thick Al layer. To achieve different degrees of crystallographic ordering, the samples are annealed at temperatures T_a of 300°C, 350°C, 400°C, 450°C, 475°C and 500°C. The detailed structural characterisation of the samples is discussed in detail elsewhere¹⁰ and here we just briefly summarize its results. X-ray diffraction reveals that all films are well epitaxially grown and (001) oriented. The θ - 2θ scan indicates B2 ordering, whereas annealing at higher temperatures promotes higher degree of L₂₁ ordering. Namely, no L₂₁ ordering was observed for samples annealed at 300°C and 350°C. A first change of crystallographic ordering towards L₂₁ structure occurs at 400°C and gets stronger with higher T_a ^{9,10}.

The analytical approximation for ferromagnetic layers describing the complex Kerr amplitude $\Phi_{s/p}$ for s and p polarized incident light is¹²

$$\Phi_s = \theta_s + i\epsilon_s = A_s \left(\epsilon_{yx} - \frac{\epsilon_{yz}\epsilon_{zx}}{\epsilon_d} \right) + B_s \epsilon_{zx}, \quad (1a)$$

$$\Phi_p = \theta_p + i\epsilon_p = -A_p \left(\varepsilon_{xy} - \frac{\varepsilon_{zy}\varepsilon_{xz}}{\varepsilon_d} \right) + B_p \varepsilon_{xz}, \quad (1b)$$

where $\theta_{s/p}$ is the Kerr rotation and $\epsilon_{s/p}$ is the Kerr ellipticity. $A_{s/p}$ and $B_{s/p}$ are the weighting optical factors, being even and odd functions of the angle of incidence (AoI), respectively. The elements ε_{ij} of the permittivity tensor ε of the magnetized crystal can be described with the use of the Einstein summation as

$$\varepsilon_{ij} = \varepsilon_{ij}^{(0)} + K_{ijk}M_k + G_{ijkl}M_kM_l, \quad (2)$$

where M_k , M_l are the components of normalized magnetization \mathbf{M} . $\varepsilon_{ij}^{(0)}$ are the components of the permittivity tensor in 0th order in \mathbf{M} . K_{ijk} and G_{ijkl} are the components of the linear and quadratic MO tensors \mathbf{K} and \mathbf{G} , respectively²². In the case of the cubic crystal structure

$$\varepsilon_{ij}^{(0)} = \delta_{ij}\varepsilon_d, \quad K_{ijk} = \varepsilon_{ijk}K, \quad (3a)$$

$$G_{iiii} = G_{11}, \quad G_{iiij} = G_{12}, \quad i \neq j, \quad (3b)$$

$$G_{1212} = G_{1313} = G_{2323} = G_{44}, \quad (3c)$$

with δ_{ij} and ε_{ijk} being the Kronecker delta and the Levi-Civita symbol, respectively. The quadratic MO parameters G_{11} and G_{12} can not be separated and they contribute to MOKE signal as $G_s = G_{11} - G_{12}$. From Eqs. (1)-(3), a measurement algorithm that separates LMOKE and two constituent QMOKE spectra Q_s and Q_{44} has been derived for (001)-oriented films and in-plane magnetization being^{20,21}

$$\begin{aligned} \text{LMOKE} &= \Phi_{s/p}^{\mu=90^\circ} - \Phi_{s/p}^{\mu=270^\circ} \\ &= \pm 2B_{s/p}K, \quad \alpha = \text{arb. angle.} \end{aligned} \quad (4a)$$

$$\begin{aligned} Q_s &= \Phi_{s/p}^{\mu=45^\circ} + \Phi_{s/p}^{\mu=225^\circ} - \Phi_{s/p}^{\mu=135^\circ} - \Phi_{s/p}^{\mu=315^\circ} \\ &= \pm 2A_{s/p} \left(G_s - \frac{K^2}{\varepsilon_d} \right), \quad \alpha = 45^\circ. \end{aligned} \quad (4b)$$

$$\begin{aligned} Q_{44} &= \Phi_{s/p}^{\mu=45^\circ} + \Phi_{s/p}^{\mu=225^\circ} - \Phi_{s/p}^{\mu=135^\circ} - \Phi_{s/p}^{\mu=315^\circ} \\ &= \pm 2A_{s/p} \left(2G_{44} - \frac{K^2}{\varepsilon_d} \right), \quad \alpha = 0^\circ. \end{aligned} \quad (4c)$$

The sample orientation α is defined as angle between [100] crystallographic direction of Co_2MnSi and x axis of sample coordinate system. Magnetization \mathbf{M} lies in-plane and its direction is defined by angle μ , being an angle between \mathbf{M} and x -axis of the sample coordinate system (see supplemental material I²³). A detailed description and derivation of the measurement algorithm can be found in Ref.²¹. Finally, note that to apply the measurement algorithm according to Eqs. (4a)-(4c), the sample must be in full magnetic saturation for every in-plane direction of the external magnetic field. The magnetic characterization of the studied samples can be found in the supplemental material II²³.

The LMOKE and QMOKE spectra presented in Figs. 1(a)-(f) were obtained from an in-house built MOKE spectroscopy setup²⁰ at room temperature with

p -polarized incident beam and using an in-plane magnetic field of 300 mT. The spectra of LMOKE rotation θ_p and ellipticity ϵ_p , measured according to Eq. (4a), are displayed in Figs. 1(a) and (b), respectively. Here, we observe no substantial change of peak position with T_a , but the change of the amplitude with T_a is well pronounced. In Figs. 1(c) and (d), we show Q_s spectra of θ_p and ϵ_p (measured according to Eq. (4b)), respectively. The spectra exhibit rapid oscillations in the spectral region 0.8 - 2.0 eV, being surprising for metallic materials. Note that the amplitude of those oscillations does depend strongly on T_a . Furthermore, a new peak arises in the θ_p spectra of Q_s at a photon energy of 2.2 eV and in the ϵ_p spectra of Q_s at a photon energy of 2.4 eV for higher T_a values. Finally in Figs. 1(e) and (f), we show the Q_{44} spectra of θ_p and ϵ_p (measured according to Eq. (4c)), respectively. Again, we observe a set of rapid oscillations in the spectral range 0.8 - 3.4 eV, where the amplitude of the peaks is proportional to T_a . Also, the formation of a new peak with higher T_a is detectable in the θ_p spectra of Q_{44} at a photon energy of 4.5 eV and in the ϵ_p spectra of Q_{44} at a photon energy of 4.4 eV. The supplemental data files in Ref.²⁴ provide all MOKE spectra presented in Fig. 1.

The dependence of the MOKE spectra on T_a can be used as a tool for comparison of the amount of L2₁ ordering in Co_2MnSi Heusler compounds. For all MOKE spectra, we approximated the dependence on T_a by linear function at each photon energy. In the peaks of QMOKE spectra, such approximation describe the experimental data very well. Figures 2 (a) and (b) present the value of this linear slope m plotted against the photon energy for θ_p and ϵ_p , respectively. In the insets of Figs. 1(a)-(d), we exemplarily present this dependence on T_a together with a linear fit (red line) at photon energies with the highest slope m . The supplemental data files in Ref.²⁵ then provide set of such a graphs for the rest of photon energies. The overall highest slope m can be identified for ϵ_p of LMOKE at 3.125 eV (ca. 396 nm), where $m = 0.142$ mdeg/K. However, m possesses high values in the whole nearby region of 2.7-4.3 eV (288-459 nm). In case of the θ_p spectra of LMOKE, the slope of the linear dependence is well pronounced in the spectral region 3.5 eV - 5.0 eV (248-355 nm) with its absolute maximum of $m = -0.084$ mdeg/K at 4.0 eV (ca. 310 nm). From the two presented QMOKE spectra, the Q_s spectra possess a higher slope almost in the whole spectral region for both θ_p and ϵ_p . Note that at 1.55 eV (800 nm) the θ_p spectra of Q_s possess a slope of $m = -0.140$ mdeg/K, being nearly equal (in absolute quantities) to the overall highest slope value of all MOKE spectra. Although Q_s requires the measurement of Kerr angles under four different \mathbf{M} directions, whereas LMOKE requires only two (compare Eqs. (4a) and (4b)), there are widely available laser diodes at 785 nm (ca. 1.53 eV) and 808 nm (ca. 1.57 eV).

To obtain spectra of MO parameters K , G_s and $2G_{44}$ to the permittivity tensor of the Co_2MnSi layer, the experimental spectra were described numerically using

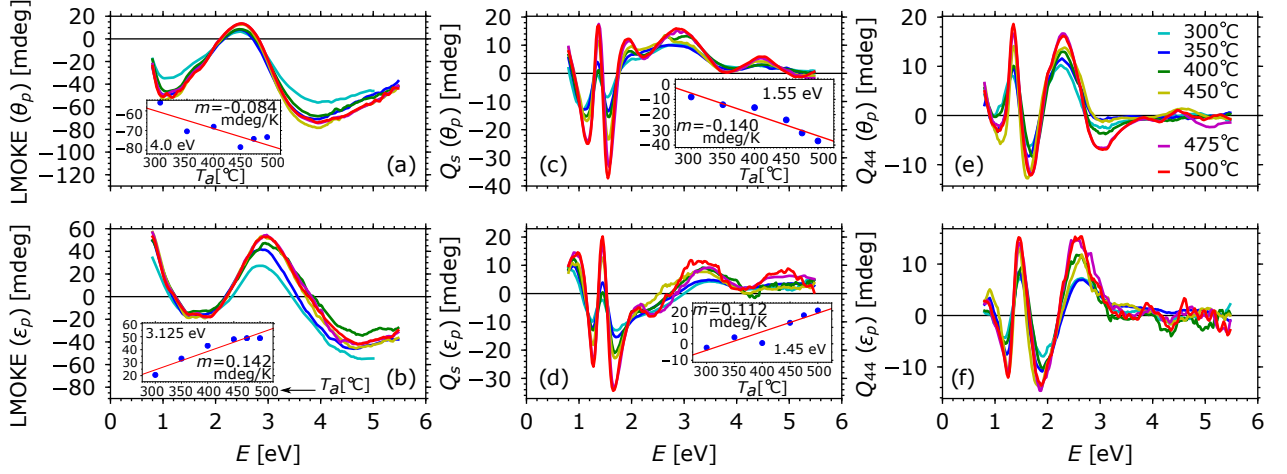


FIG. 1. LMOKE spectra of (a) θ_p , (b) ϵ_p , both measured with $\text{AoI}=45^\circ$. Q_s spectra of (c) θ_p (d) ϵ_p and Q_{44} spectra of (e) θ_p and (f) ϵ_p . Both measured with $\text{AoI}=5^\circ$. A p -polarized incident wave was used with all measurements.

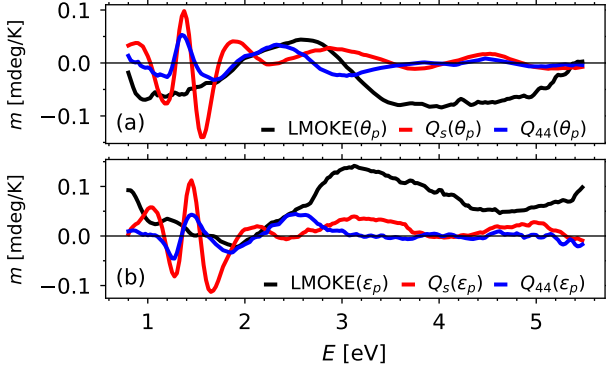


FIG. 2. Linear slope m of the dependence of the linear and quadratic MOKE signal on T_a plotted against photon energy for (a) θ_p and (b) ϵ_p of LMOKE, Q_s and Q_{44} .

4x4 Yeh matrix formalism, in which coherent propagation of the electromagnetic plane waves through a multi-layer system is considered²⁶. The MO parameters of the Co_2MnSi layers were treated as free parameters of the model and ϵ_d was obtained from the ellipsometry measurements (supplemental material III²³).

The resulted spectra of ϵ_d (permittivity in the 0th order in \mathbf{M}) and of the MO parameters K , G_s and $2G_{44}$ are shown in Fig. 3 and are accessible as supplemental data file in Ref.²⁷. All experimental spectra are accompanied by theoretical ab-initio calculations (dashed lines). For details about the ab-initio calculations, please see supplemental material IV²³ including Refs.^{28–31}. Note that all spectra shown in Fig. 3 are in the form multiplied by photon energy $E = \hbar\omega$, being actually proportional to the conductivity spectra σ_{ij} , since $\epsilon_{ij} = \delta_{ij} + i\sigma_{ij}\hbar/(\epsilon_0 E)$.

The real and imaginary part of the complex spectra of

ϵ_d are shown in Figs. 3 (a) and (b), respectively. The theoretical spectra of ϵ_d predict the major optical transitions to appear for higher energies than experimentally observed, which is apparent from Fig. 3(b). This discrepancy can be arguably attributed to the employed exchange-correlation potential, the major approximation present in the density functional theory (DFT), which still slightly overestimates distance between occupied and excited electronic states by about 0.3 eV^{32,33}.

The complex spectra of the linear MO parameter K are shown in Figs. 3 (c) and (d). Here, a new peak emerges with the presence of $L2_1$ ordering in the spectral region of 1.5 eV and 1.3 eV in real and imaginary part, respectively (note that this peak was not well observable in the LMOKE spectra itself). Although this peak is not very pronounced in the ab-initio calculations, the experimental and theoretical spectra provide otherwise good agreement.

In Figs. 3 (e) - (h), we show the complex spectra of G_s and $2G_{44}$. When compared to the spectra of Q_s and Q_{44} , described above, no new features are observed here. Although theoretical calculations of G_s are shifted in photon energies, similarly to ϵ_d spectra, amplitude and period of those oscillations are well described ab-initio. In the case of $2G_{44}$ spectra, the theory is in reasonable match with the experiment. Note that theoretical spectra of K and $2G_{44}$, for which the ab-initio calculations describe the experimental spectra well, are calculated from off-diagonal elements ϵ_{ij} ($i \neq j$) of the permittivity tensor, whereas spectra of G_s are calculated as small variation of diagonal permittivity ϵ_{ii} (see supplemental material IV²³).

In the insets of Figs. 3 (c)-(h) we present the spectra of slope m of the linear dependence of MO parameters (multiplied by photon energy E) on T_a . The highest values of m can be found for the MO parameter K , although when values of m are compared to the values of

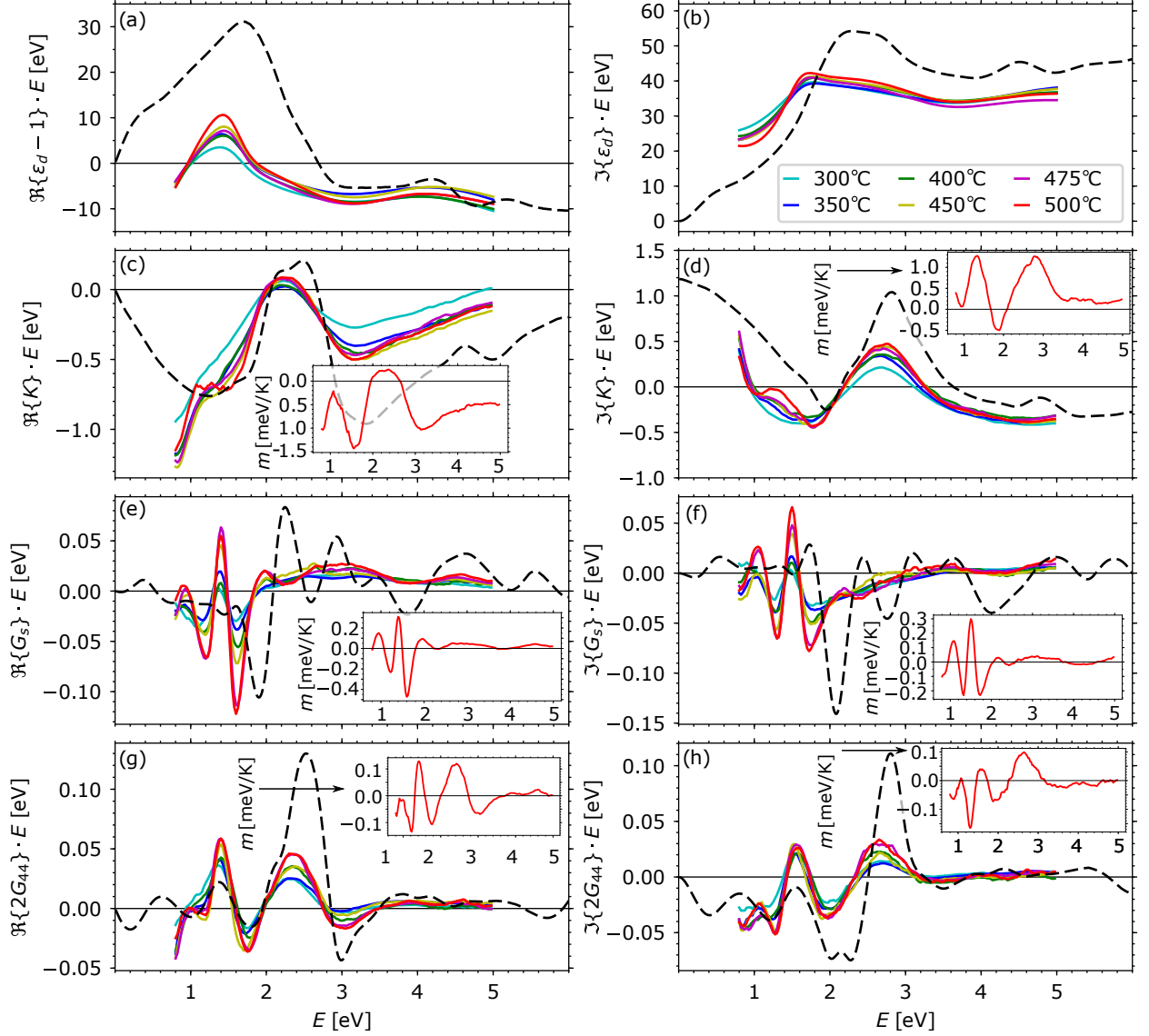


FIG. 3. Spectra of (a) real and (b) imaginary part of ε_d (permittivity of 0th order in \mathbf{M}), (c) real and (d) imaginary part of linear MO parameter K , (e) real and (f) imaginary part of quadratic MO parameter G_s , (g) real and (h) imaginary part of quadratic MO parameter $2G_{44}$. Coloured full lines are the experimental data and black dashed lines are ab-initio.

its MO parameter, it is the slope m of G_s that is most pronounced.

In conclusion, we investigated QMOKE and LMOKE spectroscopy of Co_2MnSi which undergoes a transition from B2 to L2₁ ordering provided by increasing annealing temperature T_a . We showed that the amplitude of the spectra depends on T_a and this dependence can be reasonably approximated by linear function, especially in the peaks of QMOKE spectra. We suggest the photon energies where this dependence is most pronounced and can be used as an indirect sensor of the structure ordering from an application point of view. Apart from the increase of the amplitude, several new peaks emerged with

increasing L2₁ ordering. We further extract the spectra of the MO parameters K , G_s and $2G_{44}$ and describe them ab-initio. In the case of K and $2G_{44}$ spectra, the ab-initio calculations describe the experimental spectra well. The theoretical spectra of ε_d and G_s are considerably shifted in photon energy with respect to the experimental spectra, which we attributed to the used exchange-correlation potential.

This work was supported by projects: RE1052/42-1(DFG), GA18-22102S (GACR), CZ.02.1.01/0.0/0.0/16.013/0001791(EU), CZ.02.1.01/0.0/0.0/15.003/0000487 (EU) and by EHP-CZ-ICP-1-013 (EEA grants).

- ¹T. Graf, C. Felser, and S. S. Parkin, *Prog. Solid State Chem.* **39**, 1 (2011).
- ²W. H. Wang, M. Przybylski, W. Kuch, L. I. Chelaru, J. Wang, Y. F. Lu, J. Barthel, H. L. Meyerheim, and J. Kirschner, *Phys. Rev. B* **71**, 144416 (2005).
- ³Y. Sakuraba, J. Nakata, M. Oogane, H. Kubota, Y. Ando, A. Sakuma, and T. Miyazaki, *Jpn. J. Appl. Phys.* **44**, 1100 (2005).
- ⁴M. Jourdan, J. Minár, J. Braun, A. Kronenberg, S. Chadov, B. Balke, A. Gloskovskii, M. Kolbe, H. Elmers, G. Schönhense, H. Ebert, C. Felser, and M. Kläui, *Nat. Commun.* **5**, 3974 (2014).
- ⁵S. Picozzi, A. Continenza, and A. J. Freeman, *Phys. Rev. B* **66**, 094421 (2002).
- ⁶S. Fuji, S. Sugimura, S. Ishida, and S. Asano, *J. Phys.: Condens. Matter* **2**, 8583 (1990).
- ⁷P. J. Brown, K. U. Neumann, P. J. Webster, and K. R. A. Ziebeck, *J. Phys.: Condens. Matter* **12**, 1827 (2000).
- ⁸S. Rodan, A. Alfonsov, M. Belesi, F. Ferraro, J. T. Kohlhepp, H. J. M. Swagten, B. Koopmans, Y. Sakuraba, S. Bosu, K. Takanashi, B. Büchner, and S. Wurmehl, *Appl. Phys. Lett.* **102**, 242404 (2014).
- ⁹O. Gaier, J. Hamrle, S. J. Hermsdoerfer, H. Schultheiss, B. Hillebrands, Y. Sakuraba, M. Oogane, and Y. Ando, *J. Appl. Phys.* **103**, 103910 (2008).
- ¹⁰G. Wolf, J. Hamrle, S. Trudel, T. Kubota, Y. Ando, and B. Hillebrands, “Quadratic magneto-optical Kerr effect in Co_2MnSi ,” *J. Appl. Phys.* **110**, 043904 (2011).
- ¹¹S. Trudel, O. Gaier, J. Hamrle, and B. Hillebrands, *J. Phys. D: Appl. Phys.* **43**, 193001 (2010).
- ¹²J. Hamrle, S. Blomeier, O. Gaier, B. Hillebrands, H. Schneider, G. Jakob, K. Postava, and C. Felser, *J. Phys. D: Appl. Phys.* **40**, 1563 (2007).
- ¹³J. Hamrle, S. Blomeier, O. Gaier, B. Hillebrands, H. Schneider, G. Jakob, B. Reuscher, A. Brodyanski, M. Kopnarski, K. Postava, and C. Felser, *J. Phys. D: Appl. Phys.* **40**, 1558 (2007).
- ¹⁴P. Muduli, W. Rice, L. He, and F. Tsui, *J. Magn. Magn. Mater.* **320**, L141 (2008).
- ¹⁵P. Muduli, W. Rice, L. He, B. Collins, Y. Chu, and F. Tsui, *J. Phys.: Condens. Matter* **21**, 296005 (2009).
- ¹⁶S. Trudel, J. Hamrle, B. Hillebrands, T. Taira, and M. Yamamoto, *J. Appl. Phys.* **107**, 043912 (2010).
- ¹⁷S. Trudel, G. Wolf, J. Hamrle, B. Hillebrands, P. Klaer, M. Kallmayer, H. Elmers, H. Sukegawa, W. Wang, and K. Inomata, *Phys. Rev. B* **83**, 104412 (2011).
- ¹⁸M. Veis, L. Beran, R. Anots, D. Legut, J. Hamrle, J. Pistora, C. Sterwerf, M. Meinert, J.-M. Schmalhorst, T. Kuschel, and G. Reiss, *J. Appl. Phys.* **115**, 17A927 (2014).
- ¹⁹J. Liu, S. Qiao, S. Wang, and F. Guangsheng, *Solid State Commun.* **250**, 31 (2017).
- ²⁰R. Silber, M. Tomíčková, J. Rodewald, J. Wollschläger, J. Pištora, M. Veis, T. Kuschel, and J. Hamrle, *Phot. Nano. Fund. Appl.* **31**, 60 (2018).
- ²¹R. Silber, O. Stejskal, L. Beran, L. Cejpek, R. Antoš, T. Matalla-Wagner, J. Thien, O. Kuschel, J. Wollschläger, M. Veis, T. Kuschel, and J. Hamrle, *Phys. Rev. B* **100**, 043904 (2019).
- ²²Š. Višňovský, *Czech. J. Phys. B* **36**, 1424 (1986).
- ²³“Url for supplemental materials,” .
- ²⁴“URL for data file with MOKE spectra,” ().
- ²⁵“URL for data file with MOKE dependence on T_a at each photon energy,” ().
- ²⁶P. Yeh, *Surf. Sci.* **96**, 41 (1980).
- ²⁷“URL for data file with MO parameters spectra,” ().
- ²⁸P. Blaha, K. Schwarz, G. K. H. Madsen, D. Kvasnicka, and J. Luitz, *WIEN2K, An Augmented Plane Wave + Local Orbitals Program for Calculating Crystal Properties* (Karlheinz Schwarz, Techn. Universität Wien, Austria, 2001).
- ²⁹R. Kubo, *J. Phys. Soc. Jpn.* **12**, 570–586 (1957).
- ³⁰C. Ambrosch-Draxl and J. O. Sofo, *Comput. Phys. Commun.* **175**, 1 (2006).
- ³¹J. Hamrlová, D. Legut, M. Veis, J. Pištora, and J. Hamrle, *J. Magn. Magn. Mater.* **420**, 143 (2016).
- ³²A. J. Cohen, P. Mori-Sánchez, and W. Yang, *Science* **321**, 792 (2008).
- ³³C. J. Cramer and D. G. Truhlar, *Phys. Chem. Chem. Phys.* **11**, 10757 (2009).